Self-assembly of rutile (α-TiO$_2$) nanoclusters into nanorods in microemulsions at low temperature and their photocatalytic performance

Xuebing Li, Tanwei Li, Changzheng Wu and Zude Zhang*
*Department of Chemistry and Structure Research Laboratory, University of Science and Technology of China, Hefei, Anhui, 230026, P.R. China; *Author for correspondence (Tel.: +86-551-3607752; Fax: +86-551-3606804; E-mail: xbli@mail.ustc.edu.cn)*

Abstract

A novel method – inverse microemulsion has been developed not only for synthesizing low cost TiO$_2$ nanocrystals but also for the first time making these nanocrystals self-assemble into various nanoparticles at 85°C. By variation of the volume ratios of oil to water in reverse microemulsions, the morphologies of obtained samples turned from nanoclusters to nanospherules, then grew into nanodumbbells, and became nanorods at last. It could be observed by transmission electron microscope (TEM) directly. The resulting materials were characterized by X-ray diffraction (XRD), field emission scanning electron microscope (FESEM) and high-resolution transmission electron microscope (HRTEM). The photocatalytic activity of TiO$_2$ was tested with photodegradation of Methyl Orange (MO) in water. The catalyst consisting of nanorods showed the highest photocatalytic activity, which is due to its large surface area. Furthermore, the mechanism of self-assembly of TiO$_2$ nanocrystals was discussed in detail.

Introduction

Nanotechnology has been studied extensively in the past decade for the preparation of nanoscale structures with specific size, shape and physicochemical properties. It has also created many ways to direct the assembly of nanoparticles and one-dimensional nanoscale building blocks, such as nanotubes, nanowires, and nanorods, into novel functional superstructures (Xia et al., 2003; Rogach et al., 2002; Polleux et al., 2004; Kim et al., 2001). Among them, the application of surfactants as reverse micelles or microemulsions for the synthesis and self-assembly of nanoscale structures is one of the most widely adopted methods reported in the literature. So far it has been successfully used to prepare and control the size and shape of various nanostructures with different chemical compositions, such as barium chromate (Li et al., 1999), calcium phosphates (Walsh & Mann, 1996; Bose & Saha, 2003), barium sulfate (Hopwood & Mann, 1997), cadmium selenide (Peng et al., 2000), gold nanorods (Jana et al., 2002) etc.

On the basis of the above observation, we planned to create a self-assembled way to synthesize the rutile nanocrystals in reverse microemulsions. In fact, many studies have been conducted on the synthesis and morphology control of TiO$_2$ nanoparticles. TiO$_2$ nanoparticles are obtained via the hydrolysis of titanium salts, such as titanium (IV) chloride (Park et al., 2003), titanium(IV) sulfate (Park et al., 1996), and titanium alkyloxide (Ti(OR)$_4$) in solution (Barringer & Bowen, 1985).

Hydrolysis of $TiCl_4$ in aqueous solution can form rutile nanocrystals at relative low temperatures (Park et al., 1999; Li et al., 2002; Wang et al., 2004; Yan et al., 2005). However, this method produces only polydispersed spherical or irregularly shaped particles.

In this report, we present a method not only to synthesize rutile nanocrystals but also make them self-assemble by thermal hydrolysis of $TiCl_4$ in reverse microemulsion solutions at a relative low temperature. To confirm the effects of the crystalline size and morphologies of rutile distribution on the photocatalytic activity of prepared TiO_2, the photocatalytic activity of TiO_2 with different morphologies was tested for the photodegradation of MO.

Experimental section

Preparation and characterization

All chemical reagents used in the present experiments were obtained from commercial sources as guaranteed-graded reagents and used without further purification. For the preparation of the reverse microemulsion system, cetyltrimethylammonium bromide (CTAB) was used as the surfactant, n-hexanol as the cosurfactant, and n-heptane as the continuous oil phase. $TiCl_4$ was dissolved in the hydrochloric acid as the aqueous phase in a glovebox. The synthetic procedure was as follows: Firstly, 3.8 g CTAB, 8 ml n-hexanol, and 45 ml n-heptane were mixed under magnetic stirring and secondly 1 ml of $TiCl_4$ was dissolved in 5 ml of 4.8 M hydrochloric acid solution, making up the aqueous phase. Then, the aqueous phase was added dropwise to the oil phase, forming the clear microemulsion. All of the above steps were carried out at room temperature. The microemulsion was transferred into a 100-ml flask which was kept for 6 h at 85°C, and then the precipitate was collected at the bottom of flask. The precipitate was washed repeatedly with water and ethanol to remove the oil, surfactant, cosurfactant and acid, and then dried for 12 h in oven to obtain the final sample. We changed the volume ratios of oil to water keeping pH constant under the same condition. Respectively, the volume ratios of oil to water were 2:1, 7.5:1, 15:1 and 20:1. No further heat treatment was done for all samples.

Field emission scanning electron microscopy images were obtained on a JEOL JSM-6700F SEM. Transmission electron microscopy images were obtained on a TEM (Hitachi, Model H-800). Selected area electron diffraction (SAED) patterns were supported by TEM. X-ray diffraction (XRD) patterns were obtained by XRD using a Philips X'Pert Pro Super diffractometer equipped with graphite monochromatized CuK_α radiation. A high-resolution transmission electron microscope (TEM) image was obtained by HRTEM (JEOL-2011). The specific surface areas (SSA) of the prepared catalysts were analyzed by nitrogen adsorption at 77 K, using the BET isotherm measured on the Micromeritics ASAP 2000.

Measurement of photocatalytic activity

The Methyl Orange (MO) was used as a simulated contaminant in this work. Degradation experiments were carried out by adding 0.05 g of TiO_2 powder into an 80-ml quartz photoreactor containing 50 ml of a 40 mg l^{-1} MO solution. The concentration of the catalyst was 1 g l^{-1}. The mixture was sonicated for 5 min and stirred for 10 min in the dark in order to make adsorption of rutile entirely. The stirred suspensions were illuminated with a 300-W high-pressure Hg lamp for which the strongest emission wavelength is 365 nm. The pH of the solution is 4.50. The residual MO in the solution was analyzed by checking the absorbance at 460 nm with a UV-VIS spectrophotometer (UV-2401PC).

Results and discussion

The powder XRD pattern of the as-synthesized TiO_2 nanocrystals is shown in Figure 1. All the diffraction peaks clearly could be indexed to rutile; no other phases of TiO_2, such as anatase or brookite, could be detected via XRD.

Figure 2 shows the TEM images and their corresponding SAED patterns of the obtained samples prepared in microemulsions with various ratios of oil to water at 85°C (we scanned the negative directly in order to improve the contrast). Thermal hydrolysis of $TiCl_4$ in microemulsion with a 2:1 oil to water volume ratio produced some nanoclusters with diameter about $500 \sim 600$ nm (Figure 2(a, b)). By increasing the volume ratios of
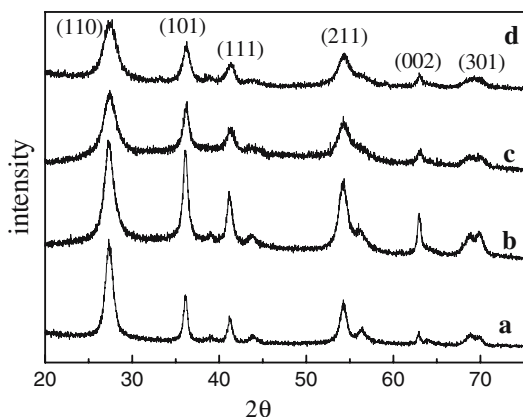
Figure 1. XRD patterns of TiO$_2$ nanocrystals prepared in reverse microemulsions with different volume ratios of oil to water at 85°C. (a) 2:1, (b) 7.5:1, (c) 15:1 (d) 20:1.
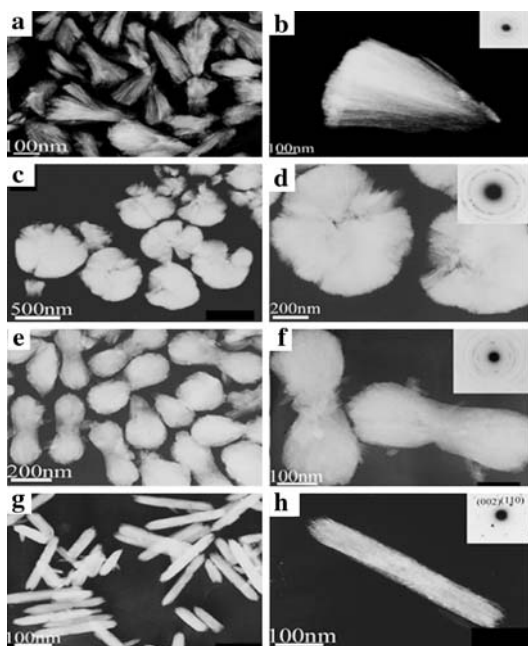

Figure 2. TEM images of TiO$_2$ synthesized in reverse microemulsions with different volume ratios of oil to water at 85°C. Every inset is its corresponding ED pattern. (a, b) 2:1, (c, d) 7.5:1, (e, f) 15:1, (g, h) 20:1.

oil to water, we found the spherule-like crystals with a diameter of 400 ~ 500 nm (Figure 2(c, d)) and the dumbbell-like nanostructural rutile about 50 ~ 80 nm in width and 300 ~ 400 nm in length (Figure 2(e, f)). When the ratio of oil to water

reached 20:1, dumbbells turned into rods about 20 ~ 30 nm in width and 200 ~ 300 nm in length (Figure 2(g, h)). Respectively, the corresponding SAED pattern is given in Figure 2(b, d, f and h). With increase of ratios of oil to water in microemulsions, it can be observed that the SAED patterns change from the relatively smooth rings to some diffuse rings and exhibit the characteristic spots at last. That's to say, the samples we prepared turn from polycrystals to single crystals gradually, which means that it has a stronger tendency to grow along a special orientation with increase of ratios of oil to water.

Figure 3 shows a high-resolution transmission electron microscope (HRTEM) image of the rutile nanorod. The surface observed in the image corresponds to the rod as indicated in an image at a low magnification (inset of Figure 3). The lattice points can be observed clearly. The distance between the adjacent lattice fringes can be assigned to the interplaner distance of rutile TiO$_2$ (110), which is $d_{110} = 3.247$ Å. The rods have therefore grown along the [001]-axis that is perpendicular to the [110]-axis, which is consistent with the SAED pattern of the rod (inset of Figure h) Meanwhile, the adjacent lattice fringes can also be assigned to the (101) which is $d_{101} = 2.490$ Å.

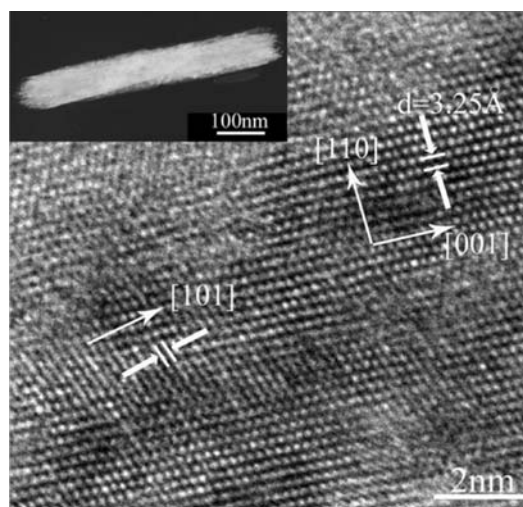In order to get more detailed microstructure of the surface, the FESEM images of the samples are

Figure 3. HR-TEM image of one of the TiO$_2$ nanorods prepared in reverse microemulsion with a 20:1 volume ratio of oil to water at 85°C.
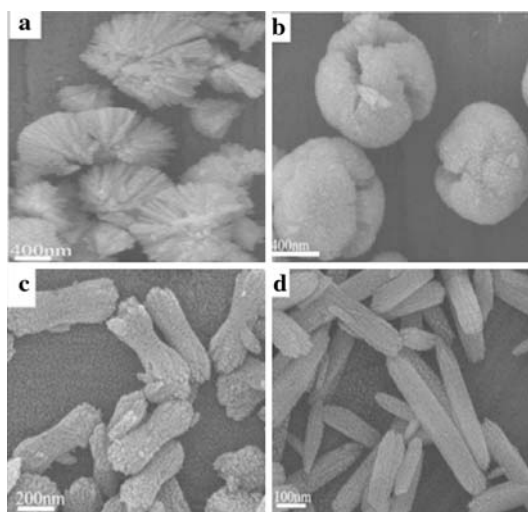
Figure 4. FE-SEM images of TiO$_2$ synthesized in reverse microemulsions with different volume ratios of oil to water at 85°C. (a) 2:1, (b) 7.5:1, (c) 15:1, (d) 20:1.

obtained that were prepared in microemulsions with various volume ratios of oil to water at 85°C (Figure 4). We could observe the variation of the morphologies of the samples clearly, which is in accordance with the TEM images (Figure 2). Meanwhile, we found the samples were made up of some small crystallites and the surfaces of the nanoparticles were scraggy, which indicates that the resulting materials are synthesized by accumulation of crystallites in a self-assembly way.

Table 1 shows the properties of rutile prepared in microemulsions with different volume ratios of oil to water. It could be found the crystallite sizes of resulting samples under different conditions are almost constant (7–8 nm) while the surface areas change a lot. It is self-assembly of these crystallites that leads to the great changes of the surface areas.

Table 1. Summary of the physicochemical properties of rutile nanocrystals prepared in microemulsions at 85°C

No	Volume ratio of oil to water	Crystallite size (nm)		Surface area (m^2/g)
		XRD*	TEM	
1	2:1	8.4	500∼600	172
2	7.5:1	7.8	400∼500	174
3	15:1	7.2	300∼400	186
4	20:1	7.0	100∼200	212

*Calculated by Scherrer formula: L $= 0.89\lambda/\beta \cos \theta$.

The photocatalytic activity of the obtained samples was detected by the degradation of the MO aqueous solution under UV irradiation (Figure 5). Methyl Orange doesn't nearly degrade if there is no rutile under irradiation of Hg light (Figure 5e). It can be seen that the degradation of MO is increased upon prolonging the irradiation time. Longer time irradiation obviously causes more degradation of MO. The optimum reactivity is observed at the sample prepared in microemulsion with a 20:1 oil to water volume ratio. The photoactivity gradually increased with further increases of ratios of oil to water, which indicates the surface area of crystals plays a key role in photocatalytic activity. Crystals that have a smaller size and larger surface area will have a good photocatalytic activity because they adsorb the MO easily.

In microemulsion solutions, surfactant molecules tend to self-assemble to form aggregates. With the difference of the ways that surfactant molecules aggregate, the various micelles will form, such as spherical or cylindrical droplets etc. Usually the spherical droplets will form in reverse microemulsion, but the shape of micelles in microemjlsion will turn from sphere to cylinder if the water in microemulsion is too little. It is known that oil surrounds water by the effect of surfactant in reverse microemulsion. If water is too little, it means a large quantity of hydrophilic groups will accumulate on the surface of water phase. In order
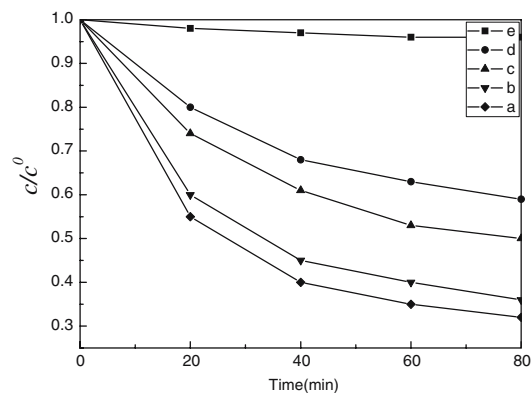

Figure 5. The photocatalytic properties of rutile TiO$_2$ samples as prepared in reverse microemulsions with different volume ratios of oil to water at 85°C under UV-light radiation with increasing irradiation time. (a) 20:1, (b) 15:1, (c) 7.5:1, (d) 2:1, (e) no rutile.
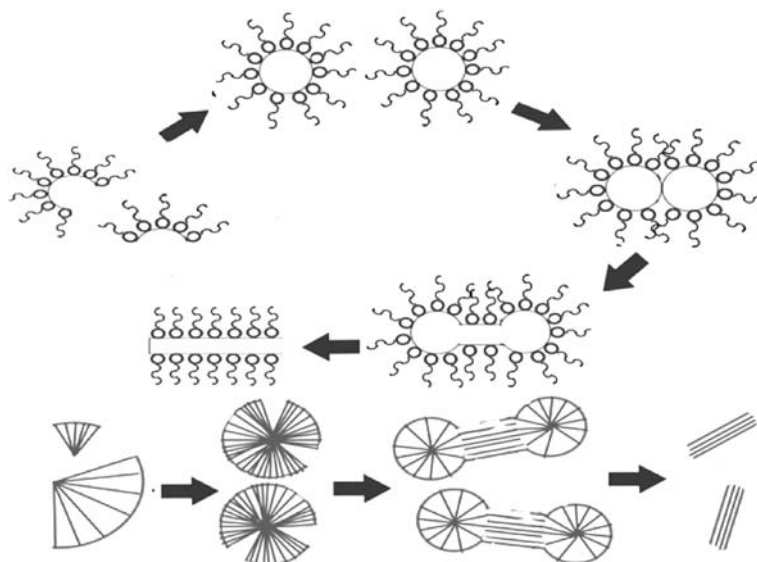
Figure 6. Proposed mechanism for self-assembly of TiO$_2$ nanoclusters into nanorods with increase of volume ratios of oil to water in reverse microemulsions.

to increase the contact area that the hydrophilic groups of surfactant come into contact with water phase, the spherical droplets grow into cylindrical droplets when the water in microemulsion decreases too much. The reason is that a cylinder that holds the same volume as a sphere will have a larger surface. It is also helpful to keep microemulsion system stable. Hence, Debye proposed a cylindrical micelle (Tadros, 1984). In our experiments, clusters and rods have been observed by TEM images (Figure 2). It indicates the existence of different droplets in reverse microemulsions. Figure 6 gives the reaction process we suggest. In this figure, the top is the process of formation of droplets in microemulsions while the bottom shows how the different morphologies of the obtained samples come into being. From Table 1, we could find the marked differences of crystals size between two ways: XRD and TEM. It could prove that self-assembly of nanocrystals has taken place in reverse microemulsions. Meanwhile, the rod-like rutile has a larger surface area than the spherule-like sample, which is in accord with the explanation about formation of cylindrical micelle. When we decreased the ratios of oil to water, the microemulsion became unstable step by step. Figure 2(a, b) shows the TEM images of obtained products prepared in reverse microemulsion with a 2:1 oil to water volume ratio. Under this condi-

tion, the structure of microemulsion has been disrupted, so we could only obtain some fan-like clusters.

Conclusions

We have demonstrated a novel method not only to prepare the rutile nanocrystallites but also make these crystals self-assemble into various nanoparticles at low temperature. By changing the volume ratios of oil to water in microemulsions, we could control the morphologies of obtained samples easily. The mechanism of self-assembly of nanoclusters into nanorods was discussed. Meanwhile, we could find the size and shape of droplets in microemulsions played a key role in controlling the morphologies of obtained products. It provides a convenient route to synthesize some special nanostructures in microemulsions, even in a predictable manner.

Acknowledgment

References

Barringer E.A. & H.K. Bowen, 1985. High-purity, monodisperse TiO₂ powders by hydrolysis of titanium tetraethoxide. 1. Synthesis and physical properties. Langmuir 1, 414–420.

Bose S. & S.K. Saha, 2003. Synthesis and characterization of hydroxyapatite nanopowders by emulsion technique. Chem. Mater 15, 4464–4469.

Hopwood J.D. & S. Mann, 1997. Synthesis of barium sulfate nanoparticles and nanofilaments in reverse micelles and microemulsions. Chem. Mater 9, 1819–1828.

Jana N.R., L.A. Gearheart, S.O. Obare, C.J. Johnson, K.J. Edler, S. Mann & C.J. Murphy, 2002. Liquid crystalline assemblies of ordered gold nanorods. J. Mater. Chem 12, 2909–2912.

Kim F., S. Kwan, J. Akana & P. Yang, 2001. Langmuir-Blodgett nanorod assembly. J. Am. Chem. Soc 123, 4360–4361.

Li M., H. Schnablegger & S. Mann, 1999. Coupled synthesis and self-assembly of nanoparticles to give structures with controlled organization. Nature 402, 393–395.

Li Y., Y. Fan & Y.J. Chen, 2002. A novel method for preparation of nanocrystalline rutile TiO₂ powders by liquid hydrolysis of TiCl₄. J. Mater. Chem. 12, 1387–1390.

Park H.K., Y.T. Moon, D.K. Kim & C.H. Kim, 1996. Formation of monodisperse spherical TiO₂ powders by thermal hydrolysis of Ti(SO₄)₂. J. Am. Ceram. Soc 79, 2727–2732.

Park I.S., S.R. Jang, J.S. Hong, R. Vittal & K.J. Kim, 2003. Preparation of composite anatase TiO₂ nanostructure by precipitation from hydrolyzed TiCl4 solution using anodic alumina membrane. Chem. Mater 15, 4633–4636.

Park S.D., Y.H. Cho, W.W. Kim & S.J. Kim, 1999. Understanding of homogeneous spontaneous precipitation for monodispersed TiO₂ ultrafine powders with rutile phase around room temperature. J. Solid State. Chem 146, 230–238.

Peng X., L. Manna, W. Yang, J. Wickham, E. Scher, A. Kadavanich & A.P. Alivisatos, 2000. Shape control of CdSe nanocrystals. Nature 404, 59–61.

Polleux J., N. Pinna, M. Antonietti & M. Niederberger, 2004. Ligand-directed assembly of preformed titania nanocrystals into highly anisotropic nanostructures. Adv. Mater 16, 436–439.

Rogach A.L., D.V. Talapin, E.V. Shevchenko, A. Kornowski, M. Haas & H. Weller, 2002. Organization of matter on different size scales: Monodisperse nanocrystals and their superstructures. Adv. Funct. Mater 12, 653–664.

Tadros T.F., 1984. Surfactants. Academic Press Inc., London.

Walsh D. & S. Mann, 1996. Chemical synthesis of microskeletal calcium phosphate in bicontinuous microemulsions. Chem. Mater 8, 1944–1953.

Wang W., B.H. Gu, L.Y. Liang, W.A. Hamilton & D.J. Wesolowski, 2004. Synthesis of rutile (α-TiO₂) nanocrystals with controlled size and shape by low-temperature hydrolysis: effects of solvent composition. J. Phys. Chem. B 108, 14789–14792.

Xia Y., P. Yang, Y. Sun, Y. Wu, B. Mayers, B. Gates, Y. Yin, F. Kim & H. Yan, 2003. One-dimensional nanostructures: synthesis, characterization, and applications. Adv. Mater.,15, 353–389.

Yan M., F. Chen, J. Zhang & M. Anpo, 2005. Preparation of controllable crystalline titania and study on the photocatalytic properties. J. Phys. Chem. B 109, 8673–8678.